ICHEP'98 #129
Submitted to Pa 1, 7
Pl 9

DELPHI 98-122 CONF 183
22 June, 1998

Measurement of the semileptonic b branching ratios and $\bar{\chi}_b$ from inclusive leptons in Z decays

Preliminary

DELPHI Collaboration

M. Calvi
Università di Milano and INFN
E. Cortina, V. Lara, F. Martínez-Vidal, J. Salt
[2] IFIC, Centro Mixto Univ. of Valencia – CSIC,
Departamento de Física Atómica, Nuclear y Molecular
Ch. de la Vaissière
[3] LPNHE, Univ. Paris VI et VII
I. Bozovic
NCSR "Demokritos", Nuclear Research Center

Abstract

In a sample of about 1.6 x 10^6 hadronic Z decays collected by the DELPHI experiment at LEP, events containing an electron or a muon were selected. The semileptonic branching ratios for primary and cascade b decays $BR(b \to \ell)$ and $BR(b \to c \to \ell)$ were measured using various techniques to separate leptons from direct or cascade b decay. The sample was enriched in b decays by means of lifetime tagging. By fitting momentum spectra of di-leptons in opposite jets, the average b mixing parameter $\bar{\chi}_b$ was also extracted.

Paper submitted to the ICHEP'98 Conference
Vancouver, July 22-29

1 Introduction

This paper presents an update of the results in [1] including data collected by the DELPHI experiment in the year 1995 and using an improved b-flavour tagging algorithm.

The semileptonic branching ratios for primary and cascade b decays BR($b \to \ell$), BR($b \to c \to \ell$) and average b mixing $\bar{\chi}_b$ are measured using momentum spectra of single lepton and di-lepton in opposite jets. The single lepton spectra are studied in a sample of pure $b\overline{b}$ events, selected by means of a b-flavour tagging algorithm. For the di-lepton sample, an enriched $b\overline{b}$ purity is obtained requiring a minimum p_t for one of the two leptons. With respect to previous analysis [2] where a global fit to several electroweak parameters was performed, there is little dependence on the partial decay widths of the Z to b and c quarks R_b and R_c, and reduced background due to misidentified hadrons and leptons from decays and punch-through of light hadrons.

Another analysis, independent from the previous one, it is also presented here. In this analysis the contributions of uds, c and b flavuors are separated in an inclusive way with a Multitag method. It has been applied to data collected with the DELPHI detector in 1994 and has been restricted to decays into muons. The results of the Multitag analysis are in agreement with those of the previous analysis, and provide an interesting cross check.

A description of the DELPHI detector is given in section 2 . The selection of the hadronic events sample is described in section 3 . A brief summary of the relevant performances of the lepton identification algorithms is given in section 4 . $b\overline{b}$ event selection using a b-flavour tagging algorithm is described in section 5. The results of the first analysis are presented in section 6, and the Multitag analysis is described in section 7.

2 The DELPHI Detector

The DELPHI detector has been described in detail in ref. [3]. Only the details relevant to this analysis are mentioned here.

In the barrel region, the charged particle tracks are measured by a set of cylindrical tracking detectors whose axes are parallel to the 1.2 T solenoidal magnetic field and to the beam direction. The time projection chamber (TPC) is the main tracking device. The TPC is a cylinder with a length of 3 m, an inner radius of 30 cm and an outer radius of 122 cm. Tracks are reconstructed using up to 16 space points in the region $39^\circ < \theta < 141^\circ$, where θ is the angle with respect to the beam direction. Tracks can be reconstructed using at least 4 space points down to 21° and 159°.

Additional precise $R\Phi$ measurements, in the plane perpendicular to the magnetic field, are provided at larger and smaller radii by the Outer and Inner detectors respectively. The Outer Detector (OD) has five layers of drift cells at radii between 198 and 206 cm and covers polar angles from 42° to 138°. The Inner Detector (ID) is a cylindrical drift chamber having inner radius of 12 cm and outer radius of 28 cm. It contains a jet chamber section providing 24 $R\Phi$ coordinates surrounded by five layers of proportional chambers providing both $R\Phi$ and longitudinal z coordinates.

The micro-vertex detector (VD) is located between the LEP beam pipe and the ID [4]. It consists of three concentric layers of silicon microstrip detectors placed at radii of 6.3, 9.0 and 10.9 cm from the interaction region, called respectively: closer, inner and

outer layer. For all layers the microstrip detectors provide hits in the $R\Phi$-plane with a measured intrinsic resolution of about 8 μm; the inner and outer layers provide in addition measurements in the z direction, with a precision depending on the polar angle and reaching a value of 9 μm for tracks perpendicular to the modules. The polar angle coverage for charged particles hitting all three layers of the detector is $44^\circ < \theta < 136^\circ$; the closer layer coverage goes down to 25°.

The barrel electromagnetic calorimeter, HPC, covers the polar angles between 42° and 138°. It is a gas-sampling device which provides complete three dimensional charge information in the same way as a time projection chamber. Each shower is sampled nine times in its longitudinal development. Along the drift direction, parallel to the DELPHI magnetic field, the shower is sampled every 3.5 mm ; in the plane perpendicular to the drift the charge is collected by cathode pads of variable size, ranging from 2.3 cm in the inner part of the detector to 7 cm in the outer layers.

In the forward region the tracking is complemented by two sets of planar drift chambers (FCA and FCB) placed at distances of $\pm$165 cm and $\pm$275 cm from the interaction point. A lead glass calorimeter (EMF) is used to reconstruct electromagnetic energy in the forward region.

Muon identification in the barrel region is based on a set of muon chambers (MUB), covering polar angles between 53° and 127°. It consists of six active planes of drift chambers, two inside the return yoke of the magnet after 90 cm of iron (inner layer) and four outside after a further 20 cm of iron (outer and peripheral layers). The inner and outer modules have similar azimuthal coverage. The gaps in azimuth between adjacent modules are covered by the peripheral modules. Therefore a muon traverses typically either two inner layer chambers and two outer layer chambers, or just two peripheral layer chambers. Each chamber measures the $R\Phi$ coordinate with a precision of about 2-3 mm. Measuring $R\Phi$ in both the inner layer and the outer or peripheral layer determines the azimuthal angle of muon candidates leaving the return yoke within about $\pm 1^\circ$. These errors are much smaller than the effects of multiple scattering on muons traversing the iron.

In the forward region the muon identification is done using two sets of planar drift chambers (MUF) covering the angular region between 11° and 45°. The first set is placed behind 85 cm of iron and the second one behind an additional 20 cm. Each set consists of two orthogonal layers of drift chambers where the anode is read out directly and the cathode via a delay line to measure the coordinate along the wire. The resolution in both coordinates is about 4 mm.

3 Event Selection

The decays of the Z to hadrons were selected by requiring:

- a total energy of the charged particles larger than 15 % of the centre of mass energy;
- at least 7 reconstructed charged particles.

  Charged particles were accepted if: $20^\circ < \theta_{track} < 160^\circ$, their track length was larger than 30 cm, their impact parameter relative to the interaction point was less than 5 cm in the plane perpendicular to the beam direction and less than 10 cm along

the beam direction and their momentum was larger than 200 MeV/c with relative error less than 100%.

Neutral particles detected in the HPC and EMF or in the hadronic calorimeters were required to have measured energy larger than 500 MeV.

With these criteria, the efficiency to select $q\bar{q}$ events from the simulation was about 95%. All sources of background have been found to be below 0.1%. No significant differences in the acceptance between different flavours have been found.

For each event the thrust axis was calculated from all the charged and neutral particles selected as above. Only events with:

$$|\cos\theta_{thrust}| < 0.90$$

were used for the following analysis. Requiring, in addition, that all subdetectors needed for this analysis were fully functional a total of about 1030000 and 515000 Z hadronic decays are selected from the 1994 and 1995 data sample respectively. About 3800000 events are selected from a sample of $Z \to q\bar{q}$ events from simulation. Events were generated with the JETSET 7.4 event generator [5] using parton shower and string fragmentation with parameters optimized to describe the hadronic distributions as measured by DELPHI. The events thus generated were passed through the program DELSIM [6] which models the detector response and processed through the same analysis chain as the real data .

Jets were formed from the charged and neutral particles using the JADE algorithm [7] with $Y_{cut}^{min} = 0.02$. When a secondary vertex was present in a jet, the jet direction was corrected using the primary to secondary vertex direction. The transverse momentum of the lepton (p_t) was determined relative to the direction of the jet, excluding the lepton itself.

4 The Lepton Sample

4.1 Muon Identification

To identify a charged particle with momentum greater than 3 GeV/c as a muon candidate, its track was extrapolated to each of the layers of the muon chambers taking into account multiple scattering in the material and the propagation of track reconstruction errors [8]. A fit was then made between the track extrapolation and the position and direction of the hits in the muon chamber. Ambiguities with muon chamber hits associated to more than one extrapolated track were resolved by selecting the track with the best fit. The charged particle was then tagged as a muon if the fit was sufficiently good and hits were found outside the return yoke iron.

To exclude regions with poor geometrical acceptance the charged particle was accepted if its polar angle, θ_μ, was within one of the following intervals

$$0.03 < |\cos\theta_\mu| < 0.62$$
$$0.68 < |\cos\theta_\mu| < 0.95,$$

which defined the barrel and the forward region, respectively. The muon identification efficiency was measured in $Z \to \mu^+\mu^-$ events, in the decays of taus into muons and in muons from two-photons collisions $\gamma\gamma \to \mu^+\mu^-$. A mean efficiency of 0.82 ± 0.01 was

found with little dependence on the muon momentum. Predictions of simulation agree with data, both in absolute value and in the momentum dependence, within a precision of 2.0% and 2.5% in the barrel and in the forward region respectively. An estimation of the misidentification probability was obtained by mean of a lifetime-based anti b-tag, to select a background enriched sample. After the subtraction of the muon content in the selected sample the misidentification probability was found to be $(0.53 \pm 0.03)\%$ in the barrel and $(0.34 \pm 0.06)\%$ the forward region. The ratio with the same quantity in simulated events was found to be 2.06 ± 0.12 (2.18 ± 0.16) in the barrel and 1.24 ± 0.21 (1.65 ± 0.25) in the forward region in the 1994 (1995) samples respectively. These ratios were used to reweight the simulated hadrons misidentified as muons. The hadron misidentification probability was cross checked using pions from K°_{s} and τ decays and compatible results were found.

4.2 Electron Identification

Charged particles with momenta greater than 3 GeV/c and within the good acceptance region of the HPC ($0.03 < |\cos\theta_e| < 0.72$) were accepted as electron candidates on the basis of the information from the HPC, the TPC and the Ring Imaging CHerenkov detector. Tracks were extrapolated to the HPC where showers were associated to them; the responses of the various detectors have then been analyzed by a neural network [9].

The network response was analized in a sample of simulated electrons from b and c decay, and a momentum dependent cut was defined in order to have a 65% efficiency constant over the full momentum range.

The efficiency of tagging an electron was measured in the data by means of a set of isolated electrons extracted from selected Compton events and a set of electrons produced from photons conversions in the detector. The efficiency was then compared to that of the simulated event samples. The ratio of the experimental efficiency to the simulated one was 0.92 ± 0.02 and 0.93 ± 0.02, in the 1994 and 1995 samples respectively and was then applied to the sample of electrons from the simulated $\mathrm{q\overline{q}}$ events.

The probability of tagging a hadron as an electron was measured in the data selecting a background sample by means of an anti b-tag technique in the same manner as for muons. The measured misidentification probability in data, and the ratio with the same quantity in simulated events were $(0.37 \pm 0.03)\%$ and 0.74 ± 0.06 in the 1994 sample, $(0.39 \pm 0.04)\%$ and 0.80 ± 0.08 respectively in the 1995 sample.

To reduce the contamination from electrons from photon conversions, electron candidates were removed if they were consistent with coming from a secondary vertex and carrying no transverse momentum to the direction from the primary to the secondary vertex.

4.3 The Simulated Lepton Sample

Samples of simulated events, which were processed through the same analysis chain as the data as descibed in section 3, were used to obtain reference spectra for the different sources of simulated leptons.

The b semileptonic decays to electrons and muons were simulated using the IGSW model. The model of Bauer et al. [10], which takes into account the finite mass of the produced lepton, was used for the B decays into τ's. For D decays the branching ratios were adjusted to be better in agreement with measured values [11], and obeying isospin

invariance in addition. The different semileptonic decay modes, the branching ratios for the decays to neutral pions, when not measured, were obtained imposing isospin invariance. To obtain the reference spectra with alternative models, events were reweighted according to the decay model considered. The weight was computed on the basis of the lepton momentum in the B(D) rest frame. For the central value in the results the ACCMM model is used, according to [13] . Lepton candidates were classified according to their different origin as follows:

a) direct b-decay:
$b \to \ell^- + X$,

b) "right sign" cascade decays:
$b \to \tau^- + X \to \ell^- + X$,
$b \to \bar{c} + X \to \ell^- + X$,

c) "wrong sign" cascade decays:
$b \to c + X \to \ell^+ + X$,

d) direct c-decay
$c \to \ell^+ + X$,
$c \to \tau^+ + X \to \ell^+ + X$,

e) prompt leptons from J/Ψ decays or from b or c decays, where the $c\bar{c}$ ($b\bar{b}$) pair is produced by gluon splitting,

f) misidentified or decaying hadrons.

The above classes are applied both to electrons and muons. The lepton candidates in the simulation were separated into these classes and reference (p_t,p_ℓ) distributions were obtained for the single leptons.

Di-lepton events were separated, for both the data and the simulated samples, into six categories depending on whether the two lepton candidates have the same or opposite charge and on which combination of lepton species (ee, $e\mu$, $\mu\mu$) they belonged to. Lepton pairs were used where the two leptons were separated by at least 90^o while lepton pairs coming from the same jet were omitted from the fit to avoid additional systematic uncertainties in the composition of the cascade lepton sample. In each category the simulated events were separated into groups consisting of allowed combinations of the above mentioned classes. To guarantee a reasonable number of events in each bin, the p and p_t of each lepton in the pair were combined to form one variable, the combined momentum, p_c, defined as $p_c = \sqrt{p_t^2 + \frac{p^2}{100}}$. Two-dimensional reference distributions were obtained for the chosen combinations in the variables (p_c^{min}, p_c^{max}), where p_c^{min}, (p_c^{max}) refers to the smaller (larger) of the two combined momenta.

5 b-flavour tagging

To assure a good efficiency in the following b-flavour tagging, events were considerd only in a region with good vertex detector acceptance: $|\cos\theta_{thrust}| < 0.7$. As a consequence, only barrel muon chambers were considered for single muons. About 768000 and 385000 Z hadronic decays were selected in the 1994 and 1995 data respectively.

Events were divided in two hemispheres, with respect to the thrust axis, and the primary vertex was reconstructed in each hemisphere. A combined b-flavour tagging algorithm [15] was used to select hemispheres enriched in b-hadron content, while in the opposite hemisphere the single lepton spectra were studied. This algorithm combines in a single variable several variables which are sensitive to the presence of a b-hadron. The main discriminating variable is the probability from all tracks belonging to the hemisphere to come from the primary vertex, calculated from the positively signed impact parameters of the tracks. Other variables were defined for hemispheres containing a secondary vertex, hemispheres without reconstructed secondary vertices were not considered. These variables are: the effective mass of particles included in the secondary vertex, the rapidity of tracks included in the secondary vertex with respect to the jet direction and the fraction of the charged energy of a jet included in the secondary vertex. For the cut on the combined variable used in this analysis, the following efficiencies for selecting different flavours were estimated from simulation:

$\varepsilon_b = (39.34 \pm 0.05)\%$

$\varepsilon_c = (1.87 \pm 0.02)\%$

$\varepsilon_{uds} = (0.189 \pm 0.003)\ \%$

The ε_b is quoted only for reference, since its simulated value is never used in the following. In fact the number N_b^H of tagged hemispheres which contain a b quark is estimated as:

$N_b^H = N_{tag}^H - (\varepsilon_c \times R_c + \varepsilon_{uds} \times R_{uds}) \times 2N_{had}$

where: N_{tag}^H and N_{had} are the total number of tagged hemispheres and the number of hadronic events respectively, ε_c and ε_{uds} are the efficiencies from simulation, $R_c = \Gamma_{c\bar{c}}/\Gamma_{had}$ and $R_{uds} = \Gamma_{uds}/\Gamma_{had} = 1 - \Gamma_{b\bar{b}}/\Gamma_{had} - \Gamma_{c\bar{c}}/\Gamma_{had}$ are the ratios of partial decay widths to c and uds quarks. For $\Gamma_{b\bar{b}}/\Gamma_{had}$ and for $\Gamma_{c\bar{c}}/\Gamma_{had}$ the LEP average 0.2170 ± 0.0009 and 0.1734 ± 0.0048 are used respectively [12].

The sample of events from Montecarlo simulation used to compare with data, is taken with a flavour composition calculated considering N_b^H from data and the contamination due to other flavours from simulation using ε_c, ε_{uds}.

6 Fitting Procedure and Results

Once an hemisphere has been tagged as b, leptons are studied in the opposite one. The main sources of leptons are prompt leptons and cascade decays leptons from b (a-c classes in section 4.3), plus a contribution from misidentified hadrons and leptons from decays of light hadrons in b events. A correction is applied, due to the correlation between the lifetime tag and the lepton tag. According to simulation it mainly arises from the acceptance requirements and amounts to $\rho_e = 1.003 \pm 0.005$ and $\rho_\mu = 1.017 \pm 0.005$, where ρ is the ratio between the fraction of leptons tagged in a hemisphere opposite to a b-flavour tagged one and the fraction of leptons tagged in an unbiased b hemisphere. A binned maximum likelihood fit is used to compare momentum and transverse momentum spectra of electrons and muons in data with simulation expectations.

The single lepton likelihood is multiplied by a likelihood obtained for di-leptons in opposite hemispheres, to help in separating the $\mathrm{BR}(\mathrm{b} \to \ell)$ from the $\mathrm{BR}(\mathrm{b} \to \mathrm{c} \to \ell)$ component and to extract information on the average mixing parameter $\bar{\chi}_b$. In the di-lepton sample no b-flavour tag is used, in order not to introduce any bias. The b enrichment is obtained requiring a minimum p_t for one of the two leptons. The full p_t spectra is

considered for the opposite lepton. For a cut at $p_t > 1.2\ GeV/c$ a b purity of about 88% is obtained, according to simulation.

If $B^0 - \bar{B}^0$ mixing is not considered, the main source of di-leptons having opposite charge are direct b-decays: $(\mathrm{b} \to \ell^-)(\bar{\mathrm{b}} \to \ell^+)$, but in the presence of mixing a fraction $2\bar{\chi}_b(1-\bar{\chi}_b)$ of these di-leptons have the same charge. Same charge di-leptons also arise from events with one direct b-decay and one cascade b-decay: $(\mathrm{b} \to \ell^-)(\bar{\mathrm{b}} \to \bar{\mathrm{c}} \to \ell^-)$, but due to mixing a fraction $2\bar{\chi}_b(1-\bar{\chi}_b)$ of these will enter the opposite charge class.

The results obtained in the 1994 and 1995 samples and their combination are shown in table 1, where the errors are statistical only.

	1994	1995	1994+1995
$\mathrm{BR}(\mathrm{b} \to \ell)$	0.1069 ± 0.0014	0.1060 ± 0.0019	0.1065 ± 0.0011
$\mathrm{BR}(\mathrm{b} \to \mathrm{c} \to \ell)$	0.0790 ± 0.0028	0.0790 ± 0.0039	0.0791 ± 0.0023
$\bar{\chi}_b$	0.122 ± 0.016	0.140 ± 0.022	0.128 ± 0.013

Table 1: Results of the fit to the 1994 and 1995 lepton samples and their combination. The errors are statistical only.

The Peterson fragmentation parameter [14] ϵ_b was left free in the fit. Converted into the mean fractional energy of b-flavoured hadrons it gives $\langle x_E \rangle = 0.712 \pm 0.003$, where the error is statistical only.

In figures 1 single lepton and di-lepton spectra are shown both for the single leptons and for the di-leptons. The simulation spectra are reweighted to the result of the fit.

The correlation matrix for the statistical error is shown in table 2.

	$\mathrm{BR}(\mathrm{b} \to \ell)$	$\mathrm{BR}(\mathrm{b} \to \mathrm{c} \to \ell)$	$\bar{\chi}_b$	ϵ_b
$\mathrm{BR}(\mathrm{b} \to \ell)$	1.00	-0.491	0.104	0.209
$\mathrm{BR}(\mathrm{b} \to \mathrm{c} \to \ell)$		1.00	-0.124	-0.132
$\bar{\chi}_b$			1.00	0.025
ϵ_b				1.00

Table 2: Correlation matrix of statistical uncertainties.

The following sources of systematic uncertainty have been considered.

- experimental uncertainty related to lepton measurements:

  the muon and electron identification efficiencies and the background due to hadron misidentification have been varied considering their measurement errors in the data-Montecarlo comparisons (see sections 4.1,4.2). An additional uncertainty of 2% has been considered on the efficiencies, to account for effects related to the difference in topology between the test samples used in sections 4.1,4.2 and the hadronic environment.

  The residual contamination in the electron sample due to coverted photons has been varied by 10%.

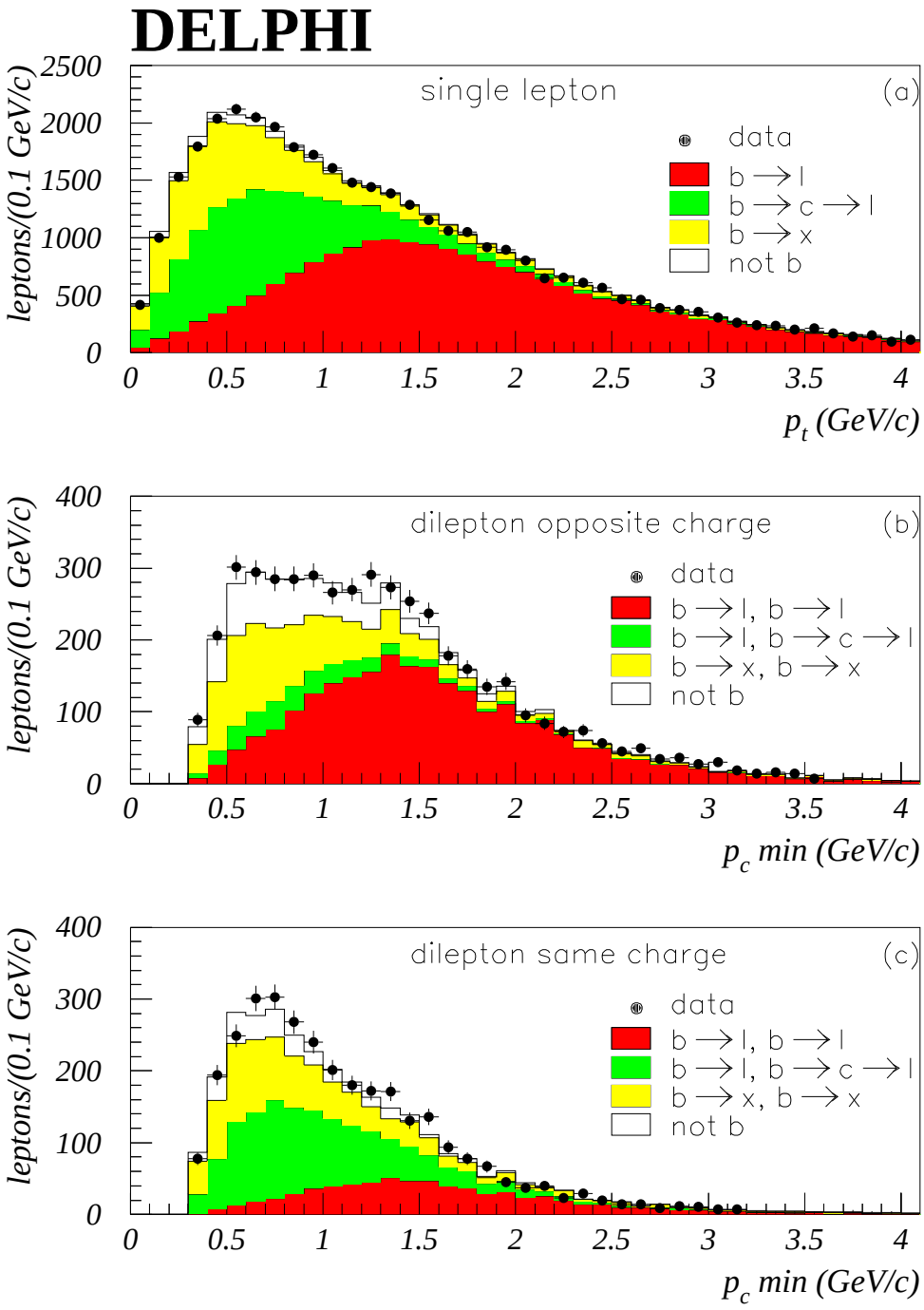

Figure 1: Comparison of data and simulation spectra. The simulation spectra are reweighted to the result of the fit. (a) Transverse momentum distribution for single electrons and muons. (b) Combined momentum distribution for di-lepton in opposite jets having opposite charge. (c) Combined momentum distribution for di-lepton in opposite jets having the same charge. In (b) and (c) the $p_c min$ refers to the minimum combined momentum of the two leptons.

Error Source	Range	ΔBR(b $\to \ell$) 10^{-2}	ΔBR(b $\to$ c $\to \ell$) 10^{-2}	$\Delta\bar{\chi}_b$ 10^{-2}
electron efficiency	$\pm 3.\%$	∓ 0.15	∓ 0.14	± 0.02
misidentified e	$\pm 8\%$	∓ 0.05	∓ 0.14	± 0.04
converted photons	$\pm 10\%$	<0.01	∓ 0.09	± 0.03
μ efficiency barrel	$\pm 2.8\%$	∓ 0.15	∓ 0.20	± 0.06
μ efficiency forward	$\pm 3.2\%$	∓ 0.03	∓ 0.02	± 0.02
misidentified μ bar.;for.	$\pm 6.5\%$;17%	∓ 0.01	∓ 0.19	± 0.05
jet direction	0.8°	$+0.05$	-0.12	+ 0.30
ε_c	$\pm 9\%$	± 0.03	∓ 0.02	± 0.03
ε_{uds}	$\pm 22\%$	± 0.01	± 0.02	∓ 0.02
$\ell - b$ correlation	$\pm 1.\%$	∓ 0.04	∓ 0.13	± 0.06
R_b	0.2170 ± 0.0009	<0.01	<0.01	<0.01
R_c	0.1734 ± 0.0048	± 0.01	± 0.01	∓ 0.01
total experimental		± 0.23	± 0.40	± 0.32
$\langle x_E(\mathrm{c})\rangle$	0.484 ± 0.008	∓ 0.02	± 0.02	± 0.04
Br(b $\to \overline{\mathrm{c}} \to \ell^-$)	$(1.62^{+0.44}_{-0.36})\%$	∓ 0.03	∓ 0.36	± 0.29
Br(b $\to \tau \to \ell$)	$(0.452 \pm 0.074)\%$	∓ 0.02	∓ 0.06	± 0.06
Br(b $\to$ J/$\psi \to \ell^+\ell^-$)	$(0.07 \pm 0.02)\%$	∓ 0.05	± 0.02	∓ 0.17
Br(c $\to \ell$)	$(9.8 \pm 0.5)\%$	∓ 0.02	∓ 0.05	± 0.05
g $\to$ c$\bar{\mathrm{c}}$	$(2.33 \pm 0.50)\%$	<0.01	<0.01	<0.01
g $\to$ b$\bar{\mathrm{b}}$	$(0.269 \pm 0.067)\%$	∓ 0.07	∓ 0.12	± 0.14
Semilept.mod.b $\to \ell$[13]	ACCMM $(^{+\mathrm{ISGW}}_{-\mathrm{ISGW}**})$	$^{-0.24}_{+0.41}$	$^{+0.35}_{-0.50}$	$^{-0.31}_{+0.50}$
Semilept.mod.c $\to \ell$[13]	ACCMM1$(^{+\mathrm{ACCMM2}}_{-\mathrm{ACCMM3}})$	$^{-0.08}_{+0.07}$	$^{-0.13}_{+0.03}$	$^{-0.30}_{+0.31}$
total models		$^{-0.27}_{+0.43}$	$^{-0.65}_{+0.52}$	$^{-0.57}_{+0.70}$

Table 3: Summary of systematic uncertainties in the analysis of single and di-lepton events. If a range is given in % it means a relative variation around the central value.

The systematic error due to the uncertainty on the b-quark direction and consequently on the lepton transverse momentum has been evaluated comparing the jet momentum direction with the direction determined by the secondary vertex in case it was successfully reconstructed. The mean difference in the jet direction was found to be 1.5°; the fit has then been performed using both methods and half difference on the results has been used as systematic error.

- experimental uncertainty related to the b-flavour tagging:

  efficiencies to tag c and uds quarks have been varied according to the errors in [15]. The correlation between the lifetime tag and the lepton tag has been varied to twice its statistical error. The partial decay widths R_b and R_c have been varied according to their measurement errors.

  The stability of the result as a function of the cut on the b-flavour tagging variable has been checked to be compatible with the corresponding statistical fluctuations.

- the modelling uncertainty related to the assumed branching ratios and to different

lepton decay models has been calculated according to [13].

The summary of systematic uncertainties is given in table 3.

In conclusion from a fit to single and di-lepton events from data collected with the DELPHI detector in 1994 and 1995, the semileptonic branching ratios BR(b $\to \ell$), BR(b $\to$ c $\to \ell$) and the average b mixing $\bar{\chi}_b$ have been measured obtaining the following results:

$$\begin{aligned} \mathrm{BR}(\mathrm{b} \to \ell) &= (10.65 \pm 0.11(stat) \pm 0.23(exp.sys.)^{-0.27}_{+0.43}(model))\% \\ \mathrm{BR}(\mathrm{b} \to \mathrm{c} \to \ell) &= (7.91 \pm 0.23(stat) \pm 0.40(exp.sys.)^{-0.65}_{+0.52}(model))\% \\ \bar{\chi}_b &= 0.128 \pm 0.013(stat) \pm 0.003(exp.sys.)^{-0.006}_{+0.007}(model) \end{aligned}$$

7 Measurement of semileptonic b decays by applying a Multitag Method

A new measurement of BR($b \to \mu$) and BR($b \to c(\bar{c}) \to \mu$) based on a multitag method over data collected with the DELPHI detector in 1994 is presented here.

In this analysis the contributions of uds, c and b flavours are separated in an inclusive way with a Multitag method. This method has the feature of using almost all the hadronic events, due to being based on a flavour deconvolution without the need for any further cuts. One important by-product of the method is a systematic and independent analysis of the misidentification probability.

The selection of the hadronic events and the muon identification is almost the same as in section 3 and 4.1 respectively.

7.1 Flavour tagging

For flavour-tagging, a multivariate method was used. This method has been described in [16] and succesfully applied on the $\Gamma_{b\bar{b}}/\Gamma_{hadr}$ determination (see [17]). This method, which tags two hemispheres per event defined with the plane perpendicular to the thrust axis, provides two important features: a) Minimal correlation between hemispheres, in particular because the event vertex is computed independently in each hemisphere and b) Direct measurement on data of tagging efficiencies and flavour compositions. These two properties are important, the former because an independent and uncorrelated tag of the hemisphere with muon identification is needed and the latter because the formalism of the analysis requires knowledge of the efficiencies and compositions.

The classification criteria is based on the so-called flavour multivariate discriminators which combine the multivariate and the confidences tag as described in reference [19]. The flavour tag is assigned by applying cuts in a priority order to the discriminators. Inside a tag, hemispheres are subdivided into categories with additional cut criteria trying to have at least one category in each flavour with maximum efficiency and the lowest possible background. In this analysis a set of six categories have been used. In 1994 due to the introduction of double sided vertex detectors a better b-tagging has been achieved. Moreover, in this analysis a good tagging performance in the charm sector is important and the cuts defining the working point has been chosen in order to optimize the efficiency.

7.2 Flavour deconvolution

The aim of flavour deconvolution is to extract the spectra of the muon variables for each flavour. It can be achieved, because the flavour composition of each category is known as a by-product of the R_b fit. The muon variable considered in this analysis is p_t (transverse momentum with respect to the jet axis excluding the muon in the definition of the jet). Other variables can be chosen under the requirement that b tagging does not depend on these variables.

The category assigned to an identified muon is the category found by the tagging in the opposite hemisphere. The aim of doing this is to avoid correlations between the hemisphere tagging and the presence of the muon. The estimated correlation between b-hemispheres, obtained as an usual correlation involving single hemisphere tag efficiency and double hemisphere tag efficiency, has been shown to be $\rho_b = 0.0176 \pm 0.0024$ [16].

The chosen observable is the number of identified muons in a given category I in an interval of p_t ($n_I^\mu(p_t)$) and, therefore at the same interval a χ^2 function can be defined as:

$$\chi^2 = \sum_I \frac{\left(n_I^\mu(p_t) - N_{hem}\left(\sum_j \varepsilon_I^j R_j D_j^\mu(p_t)\right)\right)^2}{\sigma^2\left(n_I^\mu(p_t)\right)} \tag{1}$$

where N_{hem} is the total number of hemispheres, R_j represents the fraction of flavour j in the sample, ε_I^j is the probability to classify an hemisphere of flavour j in the category I and $D_j^l(p_t)$ are candidate muon spectrum for the flavour j, normalized to one hemisphere. The fractions R_j and the elements of the classification matrix ε_I^j are provided by the R_b fit. The formula above neglects correlations between tags in opposite hemispheres.

The minimizing of this function leads to a set of three linear equations for each p_t bin whose solutions are $D_{uds}^\mu(p_t)$, $D_c^\mu(p_t)$, $D_b^\mu(p_t)$. In order to check the goodness of the method a test has been performed with Montecarlo data (see [18]).

This method of the flavour deconvolution can also be applied to other kind of particles and observables. For example, the deconvolution can be applied to all charged tracks. The distributions obtained with tracks are an interesting result by themselves. Here they are used to compute background as described in the next section.

7.3 Background extraction

In this analysis fake muons are defined as any particle identified as muon that, either is not a muon, or is a muon, but from a light hadron decay (mainly pions and kaons). Following this definition, all identified muons in uds events are fake, if it is assumed that the fraction of heavy quark production from gluon splitting is negligible.

Since the sources of background are not the same in uds, c and b events, a different misidentification probability has been evaluated for each flavour. This evaluation has required as additional inputs the fraction of different hadron species (f(π), f(K), etc.) [20] and their identification probabilities ($\alpha(\pi)$, $\alpha(K)$, etc.). The results obtained with this determination of the muon misidentification probability has been shown to be fully compatible with an independent method used in the previous analysis.

Subtracting these contaminations from the muon candidates per hemisphere, it is possible to estimate the distributions of genuine muons. In the case of the charm flavour it is only the prompt contribution and in the case of the b flavour, it is the sum of the *prompt* and *cascade* contributions.

The fig 2 compares, in simulation, the p_t distributions of the genuine muons achieved by the subtraction with the true muon distributions directly taken from simulation. It can be seen that the full spectra of genuine muons is well reproduced.

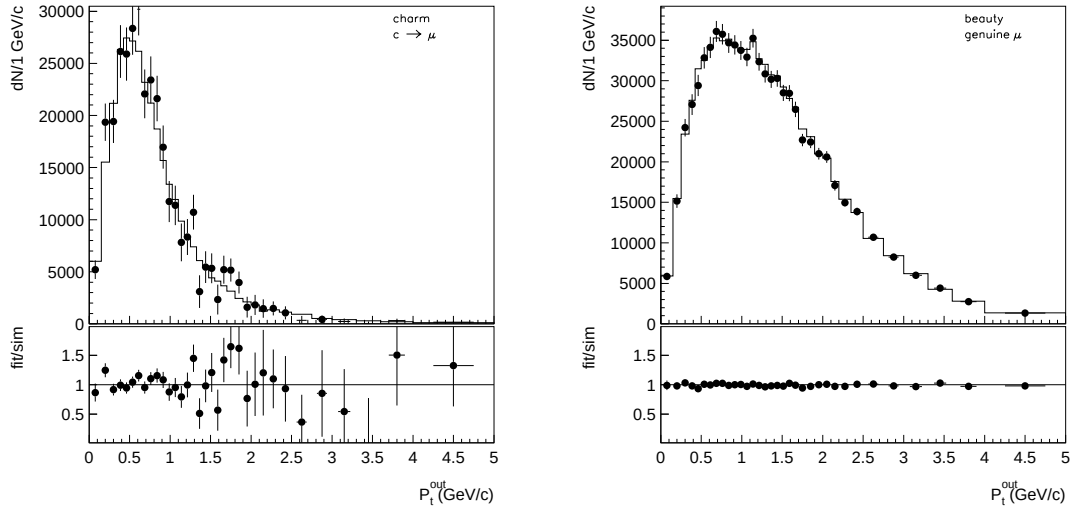

(a) p_t distribution of c genuine muons (b) p_t Distribution of b genuine muons

Figure 2: Comparison of the distributions of genuine obtained by subtraction with the true distribution in Montecarlo for the c and b flavours. The bottom part shows the ratio of the distributions.

7.4 b Semileptonic Branching Ratios from Genuine Muon Distribution

For performing the measurement of the $BR(b \to \mu)$ and $BR(b \to c(\bar{c}) \to \mu)$ a fitting strategy based on binned χ^2 fit has been applied, in which genuine muons are compared with the Montecarlo shape distributions predictions. In the fit all possible corrections due to experimental and theoretical models have been included.

The results obtained are:

$$BR(b \to \mu) = (10.57 \pm 0.14(stat))\% \quad (2)$$

$$BR(b \to c(\bar{c}) \to \mu) = (9.94 \pm 0.27(stat))\% \quad (3)$$

$$(4)$$

where the $BR(b \to c(\bar{c}) \to \mu)$ includes both the $b \to c$ and the $b \to \bar{c}$ contributions. In figure 3 the final fit is presented.

The sources of systematics errors considered are:

- Experimental uncertainties related to muon identification.

  There are basically two sources of these errors: the muon identification efficiencies and hadron misidentification. For the first a variation of 3% has been considered

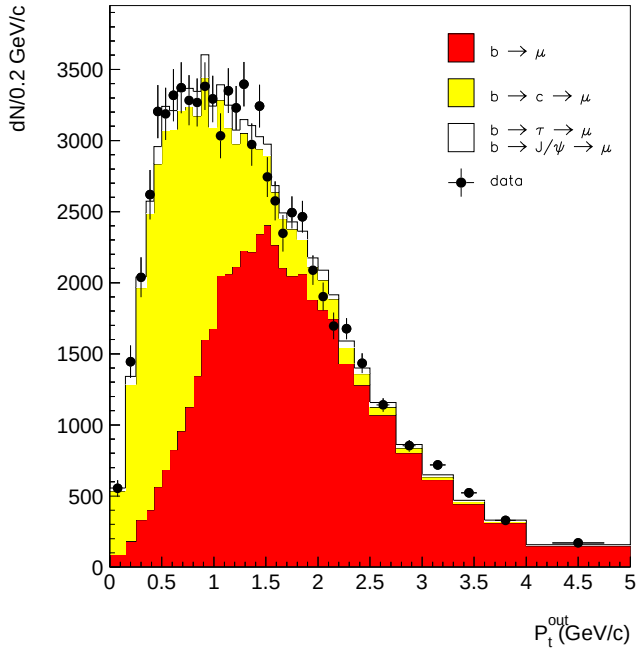

Figure 3: Final fit of muon spectrum. Several contributions to this distributios are also shown

both in barrel and forward, consistent with the first analysis. For hadron misidentification, all quantities taken from Montecarlo have been varied within 2σ in order to ensure a safe limit.

- Experimental uncertainties related to tagging.

  All tagging parameters have been varied by 2% of their nominal value (much larger than their statistical error) in an uncorrelated way. This has been done to take into account any possible correlation between them and the systematics uncertainties that have not been computed extensively. Also taken into account is the uncertainty related to rotation degenerancy, where all tagging parameters move around their central values in a correlated way. The size of this error is of the order of R_q uncertainties.

- Experimental uncertainties related to the method.

  In this category all possible uncertainties related to the method are included, such as the variation of different cuts, the choice of variables and the binning imposed for the fit.

- Theoretical uncertainties related to fragmentation.

  Fragmentation parameters are varied within 1σ. Their influence are important in the longitudinal direction with respect to jet direction , and minimal in the transverse direction.

- Theoretical uncertainties related to branching ratios.

Values from LEP Heavy Flavour Working Group have been taken and varied within 1σ. The ratios considered are: $b \to u$, $c \to l$, $b \to \tau \to l^-$, $b \to J/\psi \to l^- l^+$, $g \to b\bar{b}$ and $g \to c\bar{c}$.

- Theoretical uncertainties related to model decays.

  They are undoubtedly the main source of systematics. The choice of the models has been performed according to Lep Heavy Flavour Working Group.

The details of the systematic uncertainties are given in Table 4.
The results obtained are:

$$\begin{aligned} BR(b \to \mu) &= (10.57 \pm 0.14(stat) \pm 0.32(syst)^{-0.30}_{+0.44}(model))\% \\ BR(b \to c(\bar{c}) \to \mu) &= (9.94 \pm 0.27(stat) \pm 0.34(syst)^{+0.42}_{+0.56}(model))\% \end{aligned}$$

8 Conclusions

From a fit to single and di-lepton events from data collected with the DELPHI detector in 1994 and 1995, the semileptonic branching ratios BR(b $\to \ell$), BR(b $\to$ c $\to \ell$) and the average b mixing $\bar{\chi}_b$ have been measured obtaining the following results:

$$\begin{aligned} \mathrm{BR(b} \to \ell) &= (10.65 \pm 0.11(stat) \pm 0.23(exp.sys.)^{-0.27}_{+0.43}(model))\% \\ \mathrm{BR(b} \to \mathrm{c} \to \ell) &= (7.91 \pm 0.23(stat) \pm 0.40(exp.sys.)^{-0.65}_{+0.52}(model))\% \\ \bar{\chi}_b &= 0.128 \pm 0.013(stat) \pm 0.003(exp.sys.)^{-0.006}_{+0.007}(model) \end{aligned}$$

Another analysis, independent from the previous one, based on a Multitag method, has obtained consistent results for the $BR(b \to \mu)$ and the $BR(b \to c(\bar{c}) \to \mu)$, which provide an interesting cross check.

Error source	Range	$\Delta BR(b \to l)$	$\Delta BR(b \to c(\bar{c}) \to l)$
μ-Identification			
Id. Eff. barrel	$\pm 2.8\%$	∓ 0.258	∓ 0.210
Id. Eff. forward	$\pm 3.2\%$	∓ 0.033	∓ 0.032
μ-background			
f(π)	$(71.65 \pm 0.05)\%$	∓ 0.004	∓ 0.014
f(K)	$(16.62 \pm 0.03)\%$	∓ 0.004	∓ 0.016
f(μ-decay)	$(0.30 \pm 0.01)\%$	∓ 0.012	∓ 0.015
f($other$)	$(11.36 \pm 0.03)\%$	∓ 0.001	∓ 0.001
$\alpha(\pi)$	$(0.45 \pm 0.01\%$	∓ 0.038	∓ 0.157
$\alpha(K)/\alpha(\pi)$	(1.58 ± 0.04)	∓ 0.019	∓ 0.063
$\alpha(\mu - decay)$	$(50.8 \pm 1.00)\%$	∓ 0.007	∓ 0.057
$\alpha(other)$	$(0.05 \pm 0.004\%$	∓ 0.001	∓ 0.001
Tagging parameters			
Tag. Par. Stat.	$\pm 2\%$	± 0.134	± 0.131
Tag. Par. Rot.		± 0.034	∓ 0.049
Binning		± 0.08	± 0.08
Fragmentation			
$\langle x_E(b) \rangle$	0.702 ± 0.008	± 0.054	± 0.073
Ratios			
$Br(b \to u)$	2.6 ± 0.2 %	∓ 0.004	∓ 0.008
$Br(c \to l)$	9.8 ± 0.5 %	∓ 0.02	∓ 0.06
$Br(b \to \tau \to l^-)$	0.452 ± 0.074 %	∓ 0.016	∓ 0.07
$Br(b \to J/\psi \to l^- l^+)$	0.07 ± 0.02 %	∓ 0.047	± 0.017
$Br(g \to b\bar{b})$	0.269 ± 0.067 %	∓ 0.007	∓ 0.008
$Br(g \to c\bar{c})$	2.33 ± 0.50 %	∓ 0.001	∓ 0.002
TOTAL SYSTEMATIC(exp)		± 0.32	± 0.34
Decay Models			
$b \to l$ model	$ACCMM^{+ISGW}_{-ISGW**}$	$^{-0.285}_{+0.426}$	$^{+0.414}_{-0.537}$
$c \to l$ model	$ACCMM1^{+ACCMM2}_{-ACCMM3}$	$^{-0.083}_{+0.079}$	$^{-0.150}_{+0.058}$
Total models		$^{-0.297}_{+0.433}$	$^{+0.418}_{0.558}$

Table 4: Summary of systematic uncertainties in the Multitag analysis.

References

[1] M.Calvi and P.Ronchese *Measurement of the semileptonic b branching ratios and $\bar{\chi}_b$ from inclusive leptons in Z decays*
ICHEP'97 #415; DELPHI note 97-118 CONF100 Geneva 1997.

[2] DELPHI Collaboration, P. Abreu et al., Z. Phys. **C66** (1995) 323

[3] DELPHI Collaboration, P. Aarnio et al., Nucl. Inst. Meth. **A303** (1991) 233;
DELPHI Collaboration, P. Abreu et al., Nucl. Inst. Meth. **A378** (1996) 57

[4] N. Bingefors et al., Nucl. Inst. Meth. **A328** (1993) 447.
V. Chabaud et al., Nucl. Inst. Meth. **A368** (1996) 314.

[5] T. Sjöstrand et al., in *"Z physics at LEP 1"*, CERN 89-08, CERN, Geneva, 1989.
Comp. Phys. Comm. **39** (1986) 347.

[6] DELSIM Reference Manual, DELPHI 87-98 PROG 100, Geneva, 1989.

[7] JADE Collaboration, W.Bartel et al., Z. Phys. **C33** (1983) 23; S.Bethke et al., Phys. Lett. **B213** (1988) 235.

[8] G.R.Wilkinson *Improvements to the Muon Identification in the 94C2 Short DST Production*
DELPHI note 97-37 PHYS 690

[9] C.Kreuter *Electron Identification using a Neural Network*
DELPHI note 96-169 PHYS 658

[10] M. Bauer et al., Z. Phys. **C34** (1987) 103.

[11] Particle Data Group Eur Phys. J. **C3** (1998) 1.

[12] The LEP Collaborations ALEP, DELPHI, L3, OPAL, the LEP Electroweak Working Group and the SLD Heavy Flavour Group
A Combination of Preliminary Electroweak Measurements and Constraints on the Standard Model
CERN-PPE/97-154, 2 December 1997.

[13] The LEP Electroweak Working Group, LEPHF/98-01
ALEPH Note 98-062 PHYSIC 98-027, DELPHI 98-118 PHYS 789, L3 Note ,OPAL Technical Note TN557, July, 1998.

[14] C.Peterson et al., Phys.Rev. **D27** (1983) 105.

[15] G.J.Barker et al., *A precise measurement of the partial decay width $R_b^0 = \Gamma_{b\bar{b}}/\Gamma_{had}$*
ICHEP'98 # 123; DELPHI note 98-123 CONF 184 Geneva 1998.

[16] P. Billoir et al. Nucl. Inst. Meth. **A360** (1995) 532-558.

[17] P. Abreu et al. DELPHI Collaboration. Z. Phys. **C66** (1995) 323.

[18] J. Salt et al. Nucl. Phys. **B (Proc. Suppl.) 50** (1996) 59-62

[19] Ch. de la Vaissière and F. Martínez-Vidal *Description and performances of the DELPHI multivariate flavour tagging* DELPHI 97-134 PHYS 721.

[20] $\pi^{\pm}$, $K^{\pm}$ *and* p *and* $\bar{p}$ *production in* $Z^0 \to q\bar{q}$, $Z^0 \to b\bar{b}$ *and* $Z^0 \to u\bar{u}, d\bar{d}, s\bar{s}$, ICHEP'98 # 145; CERN EP/98-95 Submitted to Eur.Phys.Jour. C.